Appl. Phys. A (2017) 123:119
DOI 10.1007/s00339-016-0726-z

Applied Physics A
Materials Science & Processing

Theoretical study of hydrogen storage in a truncated tetrahedron hydrocarbon

Shigeru Ishikawa[1] · **Tokio Yamabe**[2]

Received: 14 October 2016 / Accepted: 22 December 2016 / Published online: 20 January 2017

Abstract A hydrocarbon molecule, having a truncated tetrahedron shape with a suitable size for the storage of a hydrogen molecule, is designed using quantum chemical methods. The molecule consists of four benzene rings bridged by six vinylene groups at the 1, 3, and 5 carbon positions of each ring, and has a stoichiometry of $C_{36}H_{24}$. The molecular geometry optimized under T_d symmetry by the B3LYP/cc-pVTZ method shows no imaginary frequencies. The size of the molecular cavity, measured by the distance between opposite vinylene groups, is 8.0 Å. The cavity has four openings along each tetrahedron face. The radius of the opening is approximately 2 Å. The system interacting with a hydrogen molecule is optimized by the MP2/cc-pVTZ method. The interaction energy is evaluated by an extrapolation method through increasing the basis set size of the hydrogen molecule from the cc-pVTZ to the cc-pV6Z with counterpoise corrections. The hydrogen molecule enters the opening by overcoming an energy barrier of +730 meV and locates at the center of the cavity with a binding energy of −140 meV. The high barrier arises from the small size of the opening. The binding energy is three times larger than that of a graphite surface and may allow hydrogen storage at milder temperatures and pressures than those required with graphite.

✉ Shigeru Ishikawa
sisikawa@keyaki.cc.u-tokai.ac.jp

[1] Department of Chemistry, School of Science, Tokai University, 4-1-1 Kitakaname, Hiratsuka 259-1292, Japan

[2] Nagasaki Institute of Applied Science, 536 Aba-machi, Nagasaki 851-0193, Japan

1 Introduction

Hydrogen tanks for fuel cell cars are required to store hydrogen with a volumetric density of 40 to 70 g/L and a gravimetric density of 5.5 to 7.5 wt% [1]. To achieve these targets, various storage methods, such as high-pressure compression, liquefaction, and materials-based storage by physisorption or chemisorption, have been investigated. Currently, high-pressure compression tanks have achieved storage densities of 17 to 25 g/L and 2.8 to 4.4 wt% under pressures between 350 and 700 bar and are implemented in cars for practical use [1]. However, to manage hydrogen safely and to save the energy required for compressing the gas, hydrogen should be stored at lower pressure and this restriction necessitates the development of materials-based storage: physisorption storage using porous materials, such as carbons and metal–organic frameworks [2], or chemisorption storage using light metals, like $LiAlH_4$ and $NaAlH_4$ [3].

Among the physisorption materials, carbon materials have been extensively studied because they take various porous structures with high stability and low weight, but their hydrogen storage density remains lower than that of high-pressure tanks even under cryogenic conditions because the interaction between a hydrogen molecule and the carbon surface is weak. A typical value of the adsorption energy of a hydrogen molecule is approximately 50 meV for graphitic materials [4, 5]. The hydrogen adsorption energy of carbon materials depends on their porous structure. Theoretical studies predict that carbon materials can increase the adsorption energy to 100 meV or higher and achieve a large storage density if their pore size is approximately 7 Å [6–8]. This prediction is consistent with the experimental observation where the hydrogen

storage in carbon materials is shown to increase with a decrease of the pore size to 7 Å or below [2].

To determine the suitable shape and size of the carbon pore for hydrogen storage, we evaluated the adsorption energy of a hydrogen molecule situated in a carbon slit, a carbon cylinder, and a carbon sphere using the Lennard–Jones potential function with reasonable parameters determined from the experiment [9, 10]. When we enclosed the hydrogen molecule in a carbon sphere with a radius of 3.37 Å, we obtained the maximum adsorption energy of 200 meV, which was approximately four times larger than that of a graphite surface. We made a circular opening on the sphere. When the opening radius was increased to 2.92 Å, the adsorption energy decreased to 150 meV but the energy barrier at the opening disappeared. We plotted the Langmuir isotherm for this case based on the eigenvalues of the adsorption potential curve and examined the occupancy of the adsorption site. The occupancy exceeded 0.5 at lower pressures than 50 bar when the temperature was below 250 K. These conditions are milder than those required for adsorption on a graphite surface.

Besides the storage conditions, the number of adsorption sites determines the storage amount. To obtain a large amount of storage in a limited volume, the adsorption sites must be distributed densely in the space; hence, the pores must be placed as close as possible to each other or they should fill the space without any gaps. This subject is related to the space-filling problem. Some regular polyhedrons can tessellate a three-dimensional space. Five polyhedrons are known to be able to tessellate such a space. However, a proper combination of two or more polyhedrons can also tessellate such a space. For example, a truncated tetrahedron can tessellate the space when it is combined with a tetrahedron [11].

In this study, we propose a new hydrocarbon molecule having a truncated tetrahedron shape with a suitable size for the storage of a hydrogen molecule. We designed this molecule using quantum chemical methods. The molecular structure is shown in Fig. 1 with the truncated tetrahedrons tessellating the space with regular tetrahedrons. The molecule consists of four benzene rings bridged by six vinylene groups, and has a stoichiometry of $C_{36}H_{24}$. We name this polyhedron hydrocarbon "tT-$C_{36}H_{24}$" as the truncated tetrahedron is abbreviated to tT according to the Conway polyhedron notation [11]. In the tessellation, each truncated tetrahedron contacts with others at the hexagonal faces and each cross section forms one of the four faces of a regular tetrahedron. We find three kinds of hydrogen binding sites for tT-$C_{36}H_{24}$. One is at the center of the truncated tetrahedron, another is the hexagonal face of the truncated tetrahedron, and the other is the inside of the tetrahedron void. If each site binds one hydrogen molecule, their occupancies will be 1, 0.5, and 0.25 for the truncated tetrahedron center, the hexagonal face, and the tetrahedron void, respectively. In this case, four hydrogen molecules will be stored per tT-$C_{36}H_{24}$ with a storage density of 1.8 wt%. If the occupancy becomes 1 for each site, nine hydrogen molecules will be stored per tT-$C_{36}H_{24}$ with a density of 4.0 wt%. In this study, we focused our investigation on the hydrogen storage at the truncated tetrahedron center. We evaluated the binding energy of a hydrogen molecule located inside tT-$C_{36}H_{24}$ and elucidated the hydrogen binding process. We did not evaluate the hydrogen binding energies of the hexagonal face and the tetrahedron void because these required an exact knowledge of the crystal structure.

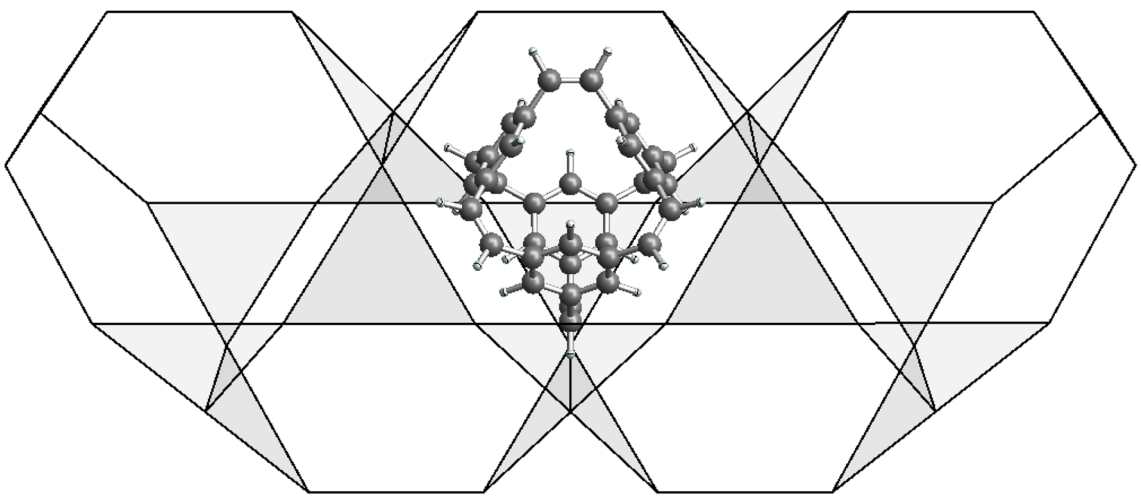

Fig. 1 The molecular structure of a truncated tetrahedron hydrocarbon with truncated tetrahedron frameworks tessellating the space with regular tetrahedrons

2 Method of calculation

We performed molecular orbital calculations using the Gaussian09 program [12]. The "tight" threshold of the program for all geometry optimization calculations was used. The isolated molecules and the interacting systems were optimized using the MP2 perturbation theory [13, 14] with the cc-pVTZ basis set [15]. We evaluated the interaction energy by an extrapolation method through increasing the basis set size of the hydrogen molecule from cc-pVTZ to cc-pV6Z [16] at the geometry obtained by the MP2/cc-pVTZ method. The basis set superposition error (BSSE) [17] of the interaction energy was corrected by the counterpoise (CP) method [18]. We did not perform the MP2 vibrational analysis of tT-$C_{36}H_{24}$ because this required large computational resources. Additionally, we performed the geometry optimization and the vibrational analysis of the molecule using the B3LYP density functional theory [19, 20] with the cc-pVTZ basis set under the "ultrafine" integration grids of the program.

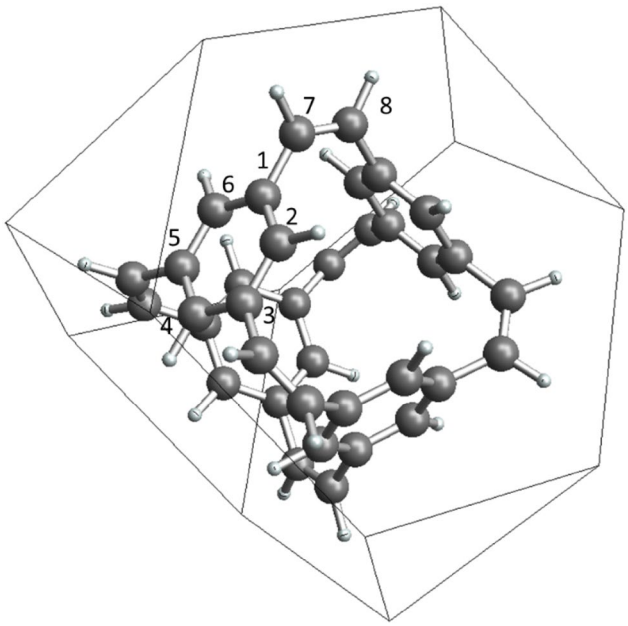

Fig. 2 The optimized structure of tT-$C_{36}H_{24}$ under T_d symmetry with a truncated tetrahedron framework

3 Results

3.1 Structure of the truncated tetrahedron hydrocarbon

The structure of tT-$C_{36}H_{24}$ under T_d symmetry was optimized by the MP2/cc-pVTZ and the B3LYP/cc-pVTZ methods and the latter provided no imaginary vibrational frequencies to the structure. The molecular structure fitted in a truncated tetrahedron framework is shown in Fig. 2. Four benzene rings of the molecule are bridged by six vinylene groups at the 1, 3, and 5 carbon positions of each ring. The truncated tetrahedron consists of four regular-triangle cross sections made by truncating the tetrahedron corners, six tetrahedron sides, and four hexagonal faces. Each cross section is occupied by a benzene ring and each tetrahedron side is occupied by a vinylene group. Each hexagonal face serves as an opening accepting a hydrogen molecule. The hydrogen atoms at the 2, 4, and 6 carbon positions of each ring surround the openings. There are three C_2 axes and four C_3 axes in the tetrahedron structure. Each C_2 axis passes the centers of the opposite vinylene groups and each C_3 axis passes the center of the benzene ring and that of the opening.

In Table 1, we show some geometrical parameters of tT-$C_{36}H_{24}$ compared with those of benzene and ethylene molecules. Each C–C bond of the benzene rings of tT-$C_{36}H_{24}$ has an equal length. The length of the C1–C2 bond of the ring (1.398 Å at the MP2/cc-pVTZ) is very close to that of the conjugated bond of the benzene molecule (1.394 Å). The length of the C7–C8 bond of the vinylene (1.340 Å) is also close to that of the double bond of the ethylene molecule (1.332 Å). The carbon atoms of tT-$C_{36}H_{24}$ are trivalent and their bond angles are approximately 120 degrees. They have an sp^2 hybridized character and exhibit an almost planar structure like the benzene and ethylene molecules. The C1–C7 bond connecting the benzene ring and the vinylene (1.479 Å) shows a single bond character like that of a cis-stilbene molecule. The B3LYP method yielded shorter lengths for the bonds having π-electrons (C1–C2 and C7–C8) and a longer length for the bond consisting of a σ bond (C1–C7) compared with the MP2 method, but the differences were small.

In Table 2, we show the sizes of the cavity and the opening of tT-$C_{36}H_{24}$. We measured the cavity size by two distances from the center of the cavity: the distance to the center of the vinylene (d_{C2}) and that to the center of the benzene ring (d_{C6}). The opening size was measured by two distances from the C_3 axis: the distance to the 2-position carbon atom (a_{C3}) and that to the hydrogen atom bonded to this atom (a_{H3}). The MP2 method yielded somewhat shorter distances compared with the B3LYP method but the differences were also small. The d_{C2} was 4.0 Å for both methods. The van der Waals radii of a carbon atom and a hydrogen atom are 1.7 and 1.2 Å, respectively, and the covalent radius of a hydrogen molecule is 0.37 Å [21]. The d_{C2} is larger than the sum of these radii (3.3 Å). Therefore, the vinylene groups do not contribute much to the hydrogen binding inside the cavity. The d_{C6} was determined as 2.82 Å with the MP2 method and 2.87 Å with the B3LYP method. These values are close

Table 1 Geometrical parameters of tT-$C_{36}H_{24}$, C_6H_6, and C_2H_4 optimized by the MP2/cc-pVTZ and B3LYP/cc-pVTZ methods

Molecule	Bond length (Å)			Bond angle (degree)		
		MP2	B3LYP		MP2	B3LYP
tT-$C_{36}H_{24}$	C1–C2	1.398	1.394	∠C1C2C3	120.9	121.1
	C7–C8	1.340	1.331	∠C2C3C4	119.1	118.9
	C1–C7	1.479	1.488	∠C1C7C8	123.6	125.6
				∠HC7C8	118.8	118.1
				∠C7C1C2	120.4	120.6
C_6H_6	C–C	1.394	1.391			
C_2H_4	C–C	1.332	1.324	∠HCC	121.3	121.7

Table 2 The cavity and opening sizes of tT-$C_{36}H_{24}$: d_{C2}, the distance from the center of the molecule to the center of the vinylene group; d_{C6}, the distance from the center of the molecule to the center of the benzene ring; a_{C3}, the distance from the C_3 axis to the peripheral carbon atom at the opening; a_{H3}, the distance from the C_3 axis to the peripheral hydrogen atom at the opening

	d_{C2}	d_{C6}	a_{C3}	a_{H3}
MP2/cc-pVTZ	4.00	2.82	2.19	1.84
B3LYP/cc-pVTZ	4.01	2.87	2.24	1.87

The unit is Å

to the optimum distance between a hydrogen molecule and an aromatic molecular plane [22, 23] or a graphite surface [4]. The four benzene rings of tT-$C_{36}H_{24}$ will cooperate to strongly bind a hydrogen molecule inside the cavity. The a_{C3} and a_{H3} were determined as 2.19 (2.24) and 1.84 (1.87) Å with the MP2 (B3LYP) method, respectively. The opening is too small to pass a hydrogen molecule without an energy barrier. The opening radius must be larger than 2.92 Å to quench the energy barrier in the case of a carbon sphere with a radius of 3.37 Å [10].

3.2 Hydrogen binding and the binding process

In Fig. 3, we show the optimized structures for binding a hydrogen molecule inside tT-$C_{36}H_{24}$. We examined three structures with changing the orientation of the hydrogen molecule: D_{2d}, C_{2v}, and C_{3v} symmetry structures. For each structure, we chose the C_n axis as the z axis and the center of mass of tT-$C_{36}H_{24}$ as the origin. We placed the hydrogen molecule along the C_n axis for the D_{2d} and C_{3v} structures and perpendicular to the C_2 axis in the C_{2v} structure. After the optimization, the center of mass of the hydrogen molecule was located at $z=0.04$ Å for the C_{2v} and C_{3v} structures. The geometry of the hydrocarbon of each structure remained almost the same as that before accepting a hydrogen molecule; the d_{C2} and d_{C6} of each structure was maintained at 4.00 and 2.82 Å, respectively. The bond length of

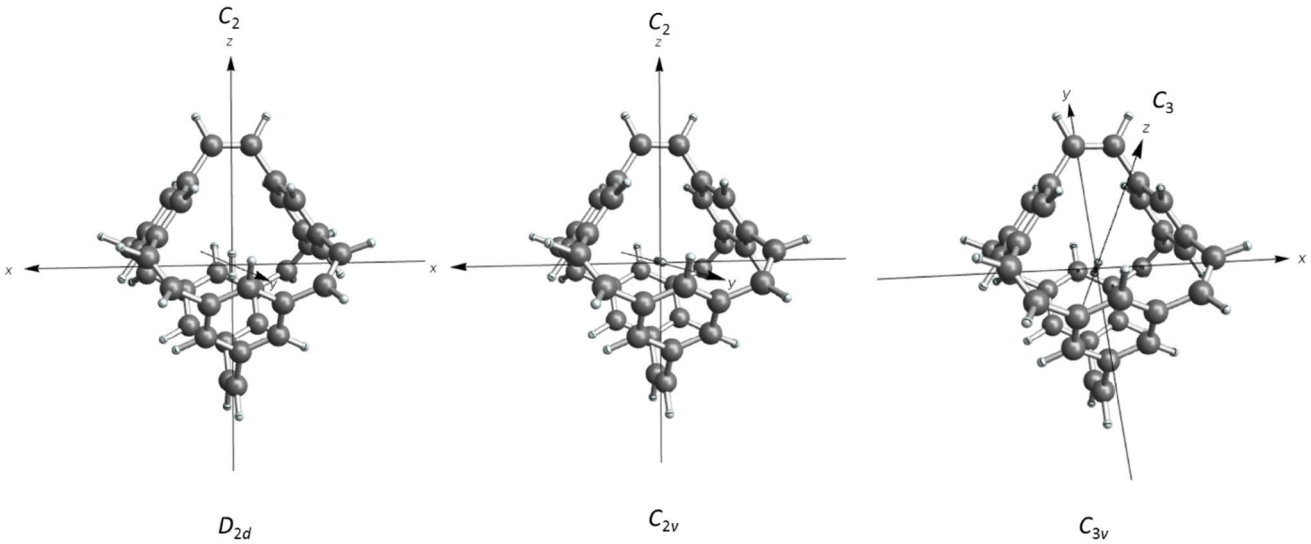

Fig. 3 The optimized structures binding a hydrogen molecule inside tT-$C_{36}H_{24}$ obtained by the MP2/cc-pVTZ method. The D_{2d}, C_{2v}, and C_{3v} symmetry forms were examined

Table 3 The interaction energy between a hydrogen molecule and tT-$C_{36}H_{24}$

Structure	No CP correction	With CP correction	Semi CBS limit
D_{2d}	−160.8	−105.5	−139.8
C_{2v}	−160.7	−105.2	−139.5
C_{3v}	−160.6	−105.1	−139.5
C_{3v}^{TS}	+716.6	+770.8	+729.1
C_{3v}^{out}	−28.4	−21.0	−26.6

The structures of the isolated molecules and the interacting systems were optimized at the MP2/cc-pVTZ level. The semi CBS limit of the energy was obtained by increasing the size of the basis set on the hydrogen molecule from the cc-pVTZ to the cc-pV6Z

the hydrogen molecule did not change much from the original length; it was stretched from 0.737 to 0.742 Å for each structure.

We show the binding energies of a hydrogen molecule in Table 3. The MP2/cc-pVTZ method evaluated the binding energy as −161 meV without the CP correction and −105 meV with the correction for each form. The energy difference between the three forms was less than 0.5 meV. The small energy differences between them allow the hydrogen molecule to rotate freely in the cavity. The BSSE given by the MP2/cc-pVTZ method became 51 meV for each form. It occupies 1/3 of the energy before the correction. This error is caused by the incompleteness of the cc-pVTZ basis set. We can decrease the BSSE by increasing the size of the basis set and eliminate the BSSE by extrapolating to the complete basis set (CBS) limit [24]. However, we could not use larger basis sets than the cc-pVTZ for tT-$C_{36}H_{24}$ because the MP2 method required large computational resources. Instead of increasing the basis set size of a whole system, we imposed large basis sets on only the hydrogen molecule. We changed the basis set of the hydrogen molecule from the cc-pVTZ to the cc-pV6Z sequentially and evaluated the CP-corrected binding energy (ΔE_{CP}) for each set. In Fig. 4, we show the plot of the ΔE_{CP} against the basis set size N, which represents the number of basis functions used to expand the valence atomic orbital that varies from 3 to 6. The partial improvement of the basis set increased the BSSE, but the ΔE_{CP} converged to a constant value as N was increased. We termed this value the "semi" CBS limit of the binding energy. To take the semi CBS limit, we assumed the exponential decrease of ΔE_{CP} with respect to N [25]:

$$\Delta E_{CP}(N) = A \exp(-BN) + C, \quad (1)$$

where A, B, and C denote the fitting parameters. In Table 3, we show the semi CBS limit of the binding energy for each structure. The energy of each structure became −140 meV. The value is approximately three times larger than that of a graphite surface (ca. −50 meV) [4] and will allow hydrogen storage at milder temperatures and pressures than graphite [10, 26].

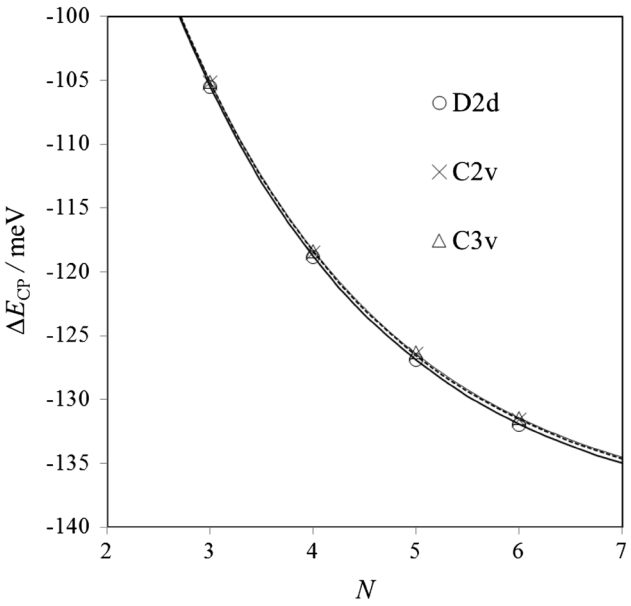

Fig. 4 The plot of the hydrogen binding energy with the CP correction (ΔE_{CP}) against the basis set size of the hydrogen molecule (N)

We examined the binding process of a hydrogen molecule moving along the C_3 axis from the outside of the opening to the inside of the cavity. In Fig. 5, we show three optimized structures appearing in the process: a structure binding a hydrogen molecule outside the opening (C_{3v}^{out}), the transition state of the process (C_{3v}^{TS}), and the C_{3v} structure binding a hydrogen molecule inside the cavity. The binding energies and the energy barrier of the hydrogen molecule for this process are shown in Table 3. For the C_{3v}^{out} structure, the hydrogen molecule was bound at $z = 5.43$ Å with a decrease of the interaction energy to −27 meV, as measured from the dissociated state. The cavity and opening sizes of this structure remained almost the same as those before the binding; the d_{C2}, d_{C6}, a_{C3}, and a_{H3} became 4.00, 2.80, 2.20, and 1.84 Å, respectively. The bond length of the hydrogen molecule (0.738 Å) was virtually the same as the original length (0.737 Å). For the C_{3v}^{TS} structure, the hydrogen molecule was located at the center of the opening ($z = 2.19$ Å) with an increase in the interaction energy to 729 meV. The incoming hydrogen molecule deformed the opening; the d_{C6}, a_{C3}, and a_{H3} became 2.86, 2.40, and 2.15 Å, respectively. Although the opening was enlarged, the radius was still smaller than that providing no barrier (>2.92 Å). The H–H bond length decreased to 0.730 Å. For the C_{3v} structure, the hydrogen molecule was bound near the center of the cavity ($z = 0.04$ Å) with a restoration of the hydrocarbon geometry and an increase of

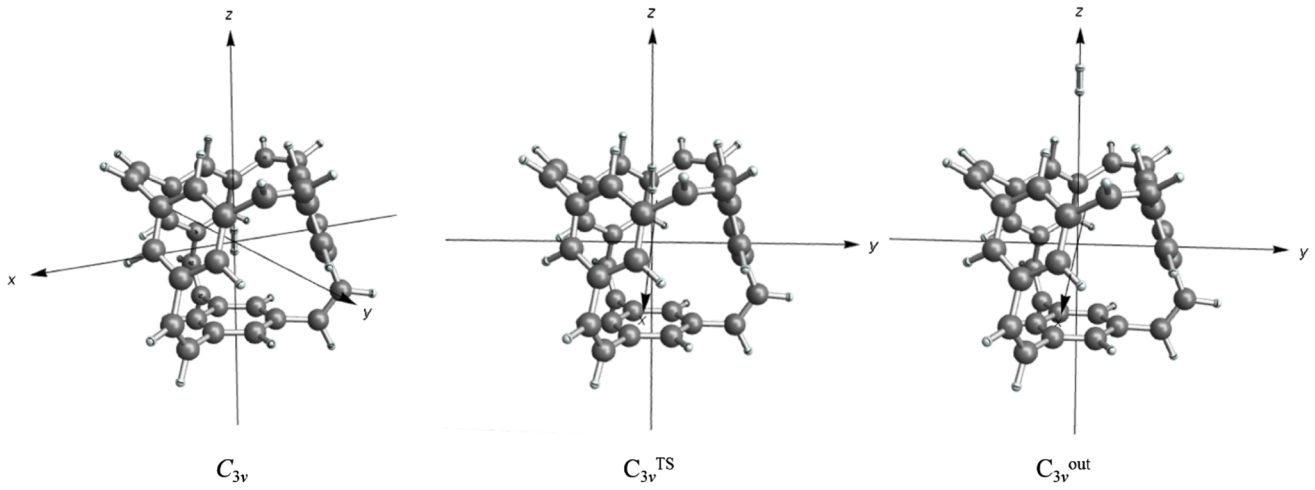

Fig. 5 The optimized structures appearing in the hydrogen binding process: $C_{3v}{}^{out}$, the structure binding a hydrogen molecule outside the opening; $C_{3v}{}^{TS}$, the transition state of the process; C_{3v}, the structure binding a hydrogen molecule inside tT-$C_{36}H_{24}$

the H–H bond length to 0.742 Å. The binding energy decreased to −140 meV.

We observed a large energy barrier, which was approximately five times larger than the binding energy inside the cavity. The barrier consists of two components: a repulsion from the opening edge and a deformation energy to enlarge the opening. The deformation energies of the hydrocarbon from the T_d structure to the $C_{3v}{}^{out}$, $C_{3v}{}^{TS}$, and C_{3v} structures were +0.7, +198, and +0.2 meV, respectively. The energy required to change the H–H bond in this process was less than 1 meV. The deformation energy from the T_d structure to the $C_{3v}{}^{TS}$ accounted for 1/4 or more of the energy barrier.

3.3 The potential energy curve

We have obtained the binding energy and the energy barrier of a hydrogen molecule accepted by tT-$C_{36}H_{24}$ using non-empirical quantum chemical methods. However, in our previous study, we derived the potential energy curve of a hydrogen molecule bound in a hollow carbon sphere with a circular opening based on the Lennard–Jones potential function [9, 10]. Here, we fit this potential curve to the obtained non-empirical results by changing the sizes of the carbon sphere and the opening.

We suppose a carbon sphere of radius d with a circular opening of radius a. The origin of the system is set at the sphere center and the z axis is drawn running through the centers of the sphere and the opening. The potential energy curve of a hydrogen molecule moving along the z axis is given by:

$$W(z,d,a) = \frac{D}{3}\left[A(z,d,a)\left(\frac{d_e}{d}\right)^{10} - B(z,d,a)\left(\frac{d_e}{d}\right)^{4}\right], \quad (2)$$

where D and d_e denote the potential depth and the optimum sphere radius, respectively. The lowest energy ($-D$) is obtained when the hydrogen molecule is located at the center of the sphere ($z=0$) if $d=d_e$ and $a=0$. The values of D and d_e are 203 meV and 3.37 Å, respectively. The detailed form of this potential function is shown in the "Appendix".

We fitted the potential curve $W(z, d, a)$ to the semi CBS limit energies of the $C_{3v}{}^{out}$, $C_{3v}{}^{TS}$, and C_{3v} structures by varying d and a. Because the $W(z, d, a)$ did not contain the deformation energy of the carbon sphere, we also fitted the $W(z, d, a)$ to the energies subtracting the deformation energies of the hydrocarbon. In Fig. 6, we show the fitted curves. The solid line denotes the curve fitted to the raw data. The fitting parameters became $d=3.10$ Å and $a=2.09$ Å. These values give approximately 40 atoms on the sphere surface. The d became close to the distance from the center of tT-$C_{36}H_{24}$ to the carbon atoms of the rings (3.2 Å). The a showed a middle value between the a_{H3} (1.84 Å) and the a_{C3} (2.19 Å) of tT-$C_{36}H_{24}$ before the hydrogen binding. The curve has the lowest minimum (−140 meV) at $z=0.1$ Å, the maximum (+732 meV) at $z=2.1$ Å, and the second lowest minimum (−33 meV) at $z=4.2$ Å. The lowest minimum and the maximum of the curve correspond to those of the non-empirical calculation. The position of the second lowest minimum of the curve is closer to the origin than that of the non-empirical result ($z=5.4$ Å) because the carbon sphere of this model does not have hydrogen atoms facing outward of the opening. The dashed line denotes the curve fitted to the data subtracting the deformation energies. The curve also reproduced the non-empirical results except for the position of the second minimum. The fitting parameters became $d=3.10$ Å and $a=2.14$ Å. The opening was enlarged by 0.04 Å and this lowered the maximum

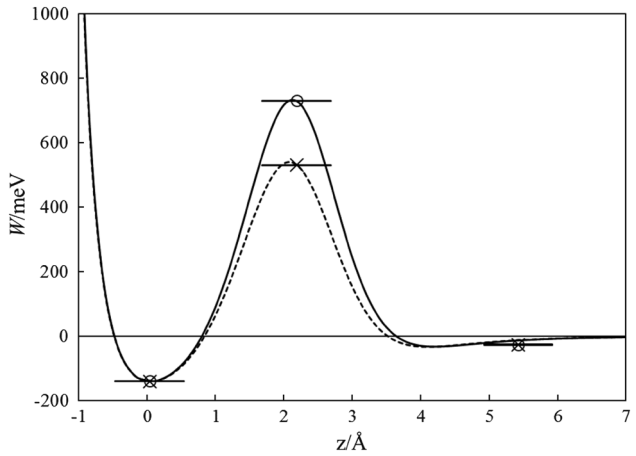

Fig. 6 The potential energy of a hydrogen molecule bound by a carbon sphere with a circular opening (W) with respect to the position of the hydrogen molecule measured from the sphere center (z). The curve was fitted to the semi CBS limit of the hydrogen binding energies of the $C_{3v}{}^{out}$, $C_{3v}{}^{TS}$, and C_{3v} structures by changing the sphere and the opening radii. The solid line denotes the curve fitted to the raw data and the dashed line denotes the curve fitted to the data subtracting the deformation energies of the hydrocarbon structures

from +732 to +539 meV. The a_{H3} and a_{C3} at the transition state were 2.15 and 2.40 Å, respectively.

In the strict sense, we should not compare the values of d and a directly with the sizes of tT-$C_{36}H_{24}$ because the $W(z, d, a)$ does not contain the interaction between a hydrogen molecule and a hydrogen atom bonded to the carbon atom in addition to the difference in the geometrical shape. Nevertheless, the discrepancies in size between the carbon sphere and tT-$C_{36}H_{24}$ are allowable if we consider the C–H group as a single atom or a united atom [27]. However, the C–H bond length cannot be ignored for such a situation as the position of the second minimum. The difference in shape can be improved using the polyhedron shape in deriving $W(z, d, a)$ [9].

4 Conclusions

We proposed a hydrogen storage material which is able to be tessellated by polyhedron nanocarbons to increase the volumetric storage density. Based on quantum chemical methods, we designed a new hydrocarbon molecule having a truncated tetrahedron shape which would fill the space together with a tetrahedron void: tT-$C_{36}H_{24}$ made by four benzene rings bridged by six vinylene groups at the 1, 3, and 5 carbon positions of each ring. We investigated its ability to store a hydrogen molecule. The size of the cavity of this molecule was 8.0 Å or less, which was close to the size of the carbon pore suitable for hydrogen storage (7 Å). The binding energy of a hydrogen molecule was evaluated by taking the semi CBS limit of the MP2 energy with the CP correction. The hydrogen molecule was bound at or near the center of the cavity with a binding energy of −140 meV, which was three times greater than that of a graphite surface, so would store hydrogen at milder temperatures and pressures than graphite. We investigated the hydrogen binding process along the C_{3v} axis running through the centers of the hexagonal opening and the benzene ring of tT-$C_{36}H_{24}$. The hydrogen molecule was loosely bound outside tT-$C_{36}H_{24}$ with a binding energy of −27 meV. The molecule overcame the energy barrier of +729 meV at the opening and entered the cavity. The high energy barrier at the opening arose from its small size. The radius of the opening measured from the C_{3v} axis to a peripheral hydrogen atom was 1.8 Å. When the hydrogen molecule approached the opening, the radius increased to 2.1 Å by consuming a deformation energy of +198 meV. To lower the energy barrier, we needed to enlarge the opening. Replacing the peripheral hydrogen atom with a carbon atom bonded to it with a nitrogen or an oxygen atom could widen the opening without provoking a large change in the electronic structure.

We examined the energy change during the hydrogen binding process using the empirical potential curve of the carbon sphere with an opening. We fitted the potential curve to the non-empirical energies by changing the sizes of the carbon sphere and the opening. We found that the empirical potential curve reproduced the non-empirical results within allowable differences in size between the carbon sphere and tT-$C_{36}H_{24}$. The non-empirical method requires a lot of time to evaluate the intermolecular interaction accurately. However, the use of the empirical potential function can save time without forfeiting the accuracy. To decrease the difference in shape, the empirical potential functions should be adapted to polyhedron shapes. These functions will assist us in designing the size and shape of the space-filling nanocarbons for hydrogen storage.

Compliance with ethical standards

Conflict of interest The authors declare that they have no conflict of interest.

Appendix

Here, we show the detailed form of the potential function of a hydrogen molecule bound in a carbon sphere of radius d with a circular opening of radius a [9, 10]. The origin of the system is set at the sphere center and the z axis is drawn running through the centers of the sphere and the opening. The potential energy curve of a hydrogen molecule moving along the z axis is given by:

$$W(z,d,a)=\frac{D}{3}\left\{\frac{1}{10(z/d)}\left[\frac{1}{\left[1-2(z/d)\cos\theta_a+(z/d)^2\right]^5}-\frac{1}{\left[1+(z/d)\right]^{10}}\right]\left(\frac{d_e}{d}\right)^{10}\right.$$
$$\left.-\frac{5}{8(z/d)}\left[\frac{1}{\left[1-2(z/d)\cos\theta_a+(z/d)^2\right]^2}-\frac{1}{\left[1+(z/d)\right]^4}\right]\left(\frac{d_e}{d}\right)^4\right\}, \tag{3}$$

where θ_a, D, and d_e denote the polar angle of the opening edge ($\theta_a=\sin^{-1}a/d$), the potential depth, and the optimum sphere radius, respectively. The lowest energy ($-D$) is obtained when the hydrogen molecule is located at the center of the sphere ($z=0$) if $d=d_e$ and $a=0$. The D and d_e are given by:

$$D=\frac{48}{5}\left(\frac{2}{5}\right)^{2/3}\pi\,\rho_s\,\sigma_{C-H_2}{}^2\,\epsilon_{C-H_2} \tag{4}$$

$$d_e=\left(\frac{5}{2}\right)^{1/6}\sigma_{C-H_2}, \tag{5}$$

where ρ_s denotes the density of the carbon surface. The $\epsilon_{C-H_2}$and σ_{C-H_2} are, respectively, the energy and distance parameters of the Lennard–Jones potential between a carbon atom and a hydrogen molecule. The hydrogen scattering experiment from the graphite surface determined their values: ϵ_{C-H_2}= 3.89 meV and σ_{C-H_2}= 2.89 Å [4]. Using the graphite surface density (0.382 Å^{-2}) for ρ_s, we obtain D = 203 meV and d_e = 3.37 Å.

References

1. Fuel Cell Technologies Office Multi-Year Research, Development, and Demonstration Plan, Sect. 3.3 Hydrogen Storage, 2012. http://energy.gov/sites/prod/files/2014/03/f12/storage.pdf, Accessed 12 Sep 2016
2. K.M. Thomas, Catal. Today **120**, 389 (2007)
3. B. Bogdanović, M. Schwickardi, J. Alloys. Compd. **253–254**, 1(1997)
4. L. Mattera, F. Rosatelli, C. Salvo, F. Tommasini, U. Valbusa, G. Vidali, Surf. Sci **93**, 515 (1980)
5. P. Bénard, R. Chahine, Langmuir **17**, 1950 (2001)
6. S. Patchkovskii, J.S. Tse, S.N. Yurchenko, L. Zhchkov, T. Heine, G. Seifert, Proc. Nat. Acad. Sci. USA **102**, 10439 (2005)
7. H. Cheng, A.C. Cooper, G.P. Pez, M.K. Kostov, P. Piotrowski, S.J. Stuart, J. Phys. Chem. B **109**, 3780 (2005)
8. B. Kuchta, L. Firlej, P. Pfeifer, C. Wexler, Carbon **48**, 223 (2010)
9. S. Ishikawa, T. Yamabe, Appl. Phys. A **114**, 1339 (2014)
10. S. Ishikawa, T. Yamabe, Appl. Phys. A **119**, 1365 (2015)
11. J.H. Conway, H. Burgiel, C. Goodman-Strass, The Symmetries of Things, 1st edn. (CRC Press, 2008), pp. 283–353
12. Gaussian 09, Revision E.01, M.J. Frisch, G.W. Trucks, H.B. Schlegel, G.E. Scuseria, M.A. Robb, J.R. Cheeseman, G. Scalmani, V. Barone, B. Mennucci, G.A. Petersson, H. Nakatsuji, M. Caricato, X. Li, H.P. Hratchian, A.F. Izmaylov, J. Bloino, G. Zheng, J.L. Sonnenberg, M. Hada, M. Ehara, K. Toyota, R. Fukuda, J. Hasegawa, M. Ishida, T. Nakajima, Y. Honda, O. Kitao, H. Nakai, T. Vreven, J.A. Montgomery Jr., J.E. Peralta, F. Ogliaro, M. Bearpark, J.J. Heyd, E. Brothers, K.N. Kudin, V.N. Staroverov, R. Kobayashi, J. Normand, K. Raghavachari, A. Rendell, J.C. Burant, S.S. Iyengar, J. Tomasi, M. Cossi, N. Rega, J.M. Millam, M. Klene, J.E. Knox, J.B. Cross, V. Bakken, C. Adamo, J. Jaramillo, R. Gomperts, R.E. Stratmann, O. Yazyev, A.J. Austin, R. Cammi, C. Pomelli, J.W. Ochterski, R.L. Martin, K. Morokuma, V.G. Zakrzewski, G.A. Voth, P. Salvador, J.J. Dannenberg, S. Dapprich, A.D. Daniels, Ö. J.B. Farkas, Foresman, J.V. Ortiz, D.J. J. Cioslowski, *Fox*. (Gaussian, Inc., Wallingford CT, 2009)
13. C. Møller, M.S. Plesset, Phys. Rev **46**, 618 (1934)
14. J.A. Pople, K. Raghavachari, H.B. Schlegel, J.S. Binkley. Int. J. Quantum Chem., Quant. Chem. Symp **S13**, 225 (1979)
15. T.H. Dunning Jr, J. Chem. Phys. **90**, 1007 (1989)
16. A.K. Wilson, T. van Mourik, T.H. Dunning Jr., J. Mol, Struct. Theochem **388**, 339 (1996)
17. T.M. Klapötke, A. Schulz, in *Quantum Chemical Methods in Main-Group Chemistry* (Wiley, Chichester, 1998), pp. 115–118
18. S.F. Boys, F. Bernardi, Mol. Phys **19**, 553 (1970)
19. A.D. Becke, J. Chem. Phys. **98**, 5648 (1993)
20. C. Lee, W. Yang, R.G. Parr, Phys. Rev. B **37**, 785 (1988)
21. A. Bondi, J. Phys. Chem **68**, 441 (1964)
22. O. Hübner, A. Glöss, M. Fichtner, W. Klopper, J. Phys. Chem. A **108**, 3019 (2004)
23. S. Ishikawa, T. Yamabe, Appl. Phys. A **99**, 29 (2010)
24. I.N. Levine, Quantum Chemistry, 4th edn, (Prentice Hall, Englewood Cliffs, 1991), pp. 603
25. M.W. Feyereisen, D. Feller, A.A. Dixon, J. Phys. Chem **100**, 2993 (1996)
26. S.K. Bhatia, A.L. Myers, Langmuir **22**, 1688 (2006)
27. A.R. Leach, *Molecular Modelling: Principles and Applications*, 2nd edn, (Pearson Education Ltd., Harlow 2001), pp. 221